DEUTSCHES ELEKTRONEN-SYNCHROTRON

DESY 93-119
August 1993

Response of Mesh-Type Photomultiplier Tubes in Strong Magnetic Fields

J. Janoth, A. Lindner, A. Walther, D. Wegener
Institut für Physik, Universität Dortmund

R.D. Appuhn, V. Korbel
Deutsches Elektronen-Synchrotron DESY, Hamburg

ISSN 0418-9833

NOTKESTRASSE 85 - 22603 HAMBURG

DESY 93-119
August 1993
ISSN 0418-9833

Response of Mesh-Type Photomultiplier Tubes in Strong Magnetic Fields

J. Janoth[1], A. Lindner, A. Walther, D. Wegener
Institut für Physik, Universität Dortmund, Germany

R. D. Appuhn, V. Korbel
Deutsches Elektronensynchrotron, Hamburg, Germany

Abstract

The performance of mesh-type photomultipliers with a diameter of 1", 1.5" and 2" respectively has been measured in magnetic fields for different angles between the field direction and the axis of the photomultiplier. Moreover the response was determined for light incident at different places of the cathode. In addition we have developed a model which describes the shape of the measured gain distributions.

1 Introduction

Recently the interest to use photodetectors in strong magnetic fields has grown [1, 2]. The proposed upgrade project of the H1 detector [3] to use a spaghetti calorimeter [4] for the measurement of electrons at small scattering angles, may serve as an example. The light output of this calorimeter amounts to 1 – 2 photoelectrons per MeV deposited energy. The need to detect this small signal combined with the requirement of precise timing information and detection of minimum ionizing particles in order to reject the high background from beam gas interactions forces to use a high gain photon-detector which has to work in a field of 1.2 Tesla. The fine mesh type phototubes recently developed by Hamamatsu [5] promise to fulfill the requirements.

These photomultipliers have a semitransparent photocathode followed by parallel planes of fine meshed dynodes. The typical mesh width is $6\,\mu m$, the mesh spacing $12\,\mu m$ and the thickness of the mesh amounts to $2\,\mu m$ [6]. In table 1 we have collected the typical parameters of the photomultiplier tubes studied [5].

2 Experimental results and their interpretation

2.1 Experimental set–up and analysis procedure

The number of photoelectrons n_p and the gain G of the dynode system has been measured with the help of a pulsed LED positioned in front of the photomultiplier. The anode-signals of the phototube are fed into a charge sensitive ADC which is gated by the pulse generator of the LED and read out by a personal computer. An aperture of 1 mm diameter is positioned between the LED and the phototube to confine the signal to a limited region of the cathode. This arrangement allows to measure local variations of the cathode efficiency and of the photomultiplier gain. The whole set-up was enclosed by a light tight box and positioned in the gap of a large dipole magnet with a homogeneous field of $B \leq 2$ Tesla. The amplification was stable during the data taking. A weak dependence of the LED output ($\leq 4\%$) on the field strength was observed. The data were corrected for this effect [7].

[1]Now at Institut für Hochenergiephysik, Universität Heidelberg, Germany

The number n_p of photoelectrons and the gain of the dynode system is derived from the mean S and variance σ_s [8] of the recorded distribution. We assume that the production of photo- and of secondary electrons is governed by Poisson statistics. In this case the number of photoelectrons is given by the expression

$$n_p = \left(1 + \sum_{k=1}^{n} \prod_{i=1}^{k} \delta_i^{-1}\right) \times \left(\frac{\sigma_s}{S}\right)^{-2} \tag{1}$$

where n is the number of dynodes and δ_i is the amplification of the dynode i.

Since in our set-up the voltage between succeeding dynodes is equal, we assume a constant amplification δ for all dynodes. Hence we get

$$n_p = \left(\frac{S}{\sigma_s}\right)^2 \times \frac{\delta}{\delta - 1} \tag{2}$$

The gain is given by

$$G = \delta^n = \frac{S \times Q}{n_p \times e} \tag{3}$$

where Q is the charge per ADC channel. Combining equation (2) and (3) allows to determine G and n_p iteratively. Further details of the set-up and the analysis procedure are given in reference [7].

2.2 Results

The measured gain G is shown in figs. 1a-c for the three types of photomultipliers studied. The following qualitative behavior is observed. For large field strengths the gain drops exponentially. A plateau is observed for the 1" tube for $B \leq 0.4$ Tesla. For the 1.5" tube this interval is narrower and it disappears for the 2" tube. The 1" and the 2" tube thus still have an appreciable gain for the nominal field of 1.2 Tesla of the H1 detector. Note that the 1.5" tube has only 12 dynodes.

The gain varies within the sample of four 1" phototubes available for our measurements as demonstrated by fig. 2 where the average gain of the four tubes and its variance is shown. The variation amounts to 20% at 1.2 Tesla, hence - aiming for high precision - a test of all tubes in the nominal field is necessary before they are installed in the experiment.

The gain of the phototubes as a function of the angle θ between the field direction and the tube axis is plotted in fig. 3. Only a modest dependence is observed at small angles. Hence no significant gain variations are expected when the tubes are installed within a precision of a few degrees in an experiment. Two additional features are observed. At angles around 35° the gain drops steeply. The angle at which this drop starts increases with B.

Finally, the gain of the 1" tube has been measured as a function of the field B for different impact points of the photons on the cathode (fig. 4). Only a weak field dependence is observed. This changes dramatically if one plots the number of photoelectrons as a function of the impact position for different fields (fig. 5). The area of the cathode which allows efficient photon detection shrinks with increasing field strength by roughly a factor of two.

2.3 Discussion of the results

We have developed a simple model to interpret the shape of the distributions presented in figs. 1 – 4. As input of the Monte Carlo simulation we use the solution of the electron's equation of motion in the combined static electric and magnetic field. We assume that the electric field is parallel to the photomultiplier axis. The energy spectrum of the secondary electrons is supposed to follow a distribution given in [9], a parametrization of this distribution is discussed in ref. [7]. The angular distribution of the electrons leaving the dynode is isotropic [9]. We assume that the energy and the angular distribution of the secondary electrons are independent of each other.

The amplification due to a single dynode depends on the angle ϕ between the direction of the primary electron and the normal to the dynode plane. We take the parametrization of [10]

$$\delta_{real} \sim \frac{1}{cos\phi}. \quad (4)$$

The ideal amplification of a dynode is a sum of two terms describing the probability of an incoming electron to pass the dynode plane via a hole or hit a bar of the grid respectively:

$$\delta_{eff}^{id} = P_{hole}^{pr} + P_{grid}^{pr} \times \delta_{real} \times P_{hole}^{sec}(\theta, B) \quad (5)$$

where P_{hole}^{pr} is the probability of a primary electron to pass the dynode through a hole . It depends weakly on the field strength of the magnetic field (< 1%) [7].

$$P_{grid}^{pr} = 1 - P_{hole}^{pr} \quad (6)$$

The factor

$$\delta_{real} = k \times \Delta U \times \frac{1}{cos\phi} \quad (7)$$

is the real emission rate of secondary electrons from the dynode which depends on the voltage difference ΔU between two succeeding dynodes and on a material specific constant k. P_{hole}^{sec} is the probability that a secondary electron is produced at the dynode and passes it via a hole. In fig. 6 the results of the calculation of P_{hole}^{sec} , which is the most sensitive term in (5), are shown as a function of the field B. The angle θ between the field direction and the photomultiplier axis is varied in the interval $0° \leq \theta \leq 40°$.

A further reduction of the gain is due to the loss of electrons at the edges of the dynodes as the center of gravity of the electron cloud follows the direction of the magnetic field. Due to the finite transverse radius of the helix a fraction of the electrons misses the edge of the grid. This effect is largest for small magnetic fields. We have combined this effect into a factor $f(\theta, B, \Delta U)$:

$$\delta_{eff} = f(\theta, B, \Delta U) \times \delta_{eff}^{id} \quad (8)$$

The overall gain of the n-stage dynode system is given by

$$G = (\delta_{eff})^n \quad (9)$$

In fig. 7 we compare the measured gain with the model prediction. The simulations are normalized to the measurements at 0.2 Tesla by a proper chosen value of δ_{real}. The characteristic features of the measurements are reproduced. The exponential decrease is due to the decrease of P_{hole}^{sec} with increasing B. The plateau observed for $B \leq 0.4$ Tesla can be traced back to the ϕ dependence in formula (4) and to the decrease of $f(\theta, B, \Delta U)$ with decreasing B. As pointed out the latter behavior is due to the increasing radius of curvature of the electrons if the field decreases.

Also the dependence of the gain on the angle θ between the field direction and the photomultiplier axis is nicely reproduced (fig. 8). The sharp drop for large angles θ is due to the factor $f(\theta, B, \Delta U)$ which approaches zero for large angles θ since the center of gravity of the electron cloud misses the anode and the radius of curvature gets small at large fields. The slow increase of the gain at small angles can be traced back to the influence of P_{hole}^{sec} in formula (5).

3 Summary

A mesh type phototube is well suited for photon detection in strong magnetic fields, since its gain is large even at fields of 1.2 Tesla. It is insensitive to small installation uncertainties, if the angle between the tube axis and the field direction is smaller than 20°. Moreover, we achieved a qualitative understanding of the tubes sensitivity to such external parameters as magnetic field and angle θ between the field direction and the phototube axis. The model can be used to optimize operational characteristics.

Acknowledgements

We acknowledge the stimulating interest of the backward upgrade group of the H1-collaboration. The support of the workshops at Dortmund university and of the machine group at DESY made our measurements possible. The Dortmund group was supported by a grant of the Bundesmisterium für Forschung und Technologie of the Federal Republic of Germany under contract number 056DO57P(6).

References

[1] F. Takasaki et al., Nucl. Instr. Meth. **228** (1985) 369

[2] G. Finsel et al., Nucl. Instr. Meth. **A290** (1990) 450

[3] H1 Collaboration, Technical Proposal to Upgrade the Backward Scattering Region of the H1 Detector, PRC 93/02

[4] P. Sonderegger, Nucl. Instr. Meth. **A257** (1987) 523

[5] Hamamatsu Photonics Data sheet R3432-01 (1992), Data sheet R2021, Data sheet R2490

[6] S. Mordhorst, diploma thesis Hamburg 1989 (unpublished)

[7] J. Janoth, diploma thesis Dortmund 1993 (unpublished)

[8] M. Dvorak, diploma thesis Dortmund 1986 (unpublished)

[9] M. von Ardenne, Effekte der Physik, VEB Verlag, Berlin 1988

[10] L. Reimer, G. Pfefferkorn, Raster-Elektronenmikroskopie, Springer Verlag, Berlin 1973

Table:

PM Typ	R3432-01 1"	R2021 1.5"	R2490-05 2"
tube length without pins [mm]	55	85	68
tube diameter [mm]	25.4	39	68
effective cathod diameter [mm]	17	25	36
window material	borosilicate	borosilicate	borosilicate
cathode material	bialkali	bialkali	bialkali
sensitive wavelength region [nm]	300 – 650	300 – 650	300 – 650
maximum sensitivity [nm]	420	420	420
No. of dynodes	15	12	16
nominal high voltage [V]	2000	2000	2500
maximum high voltage [V]	2500	2500	2700

Table 1: Parameters of the used photomultipliers [5]

Figures:

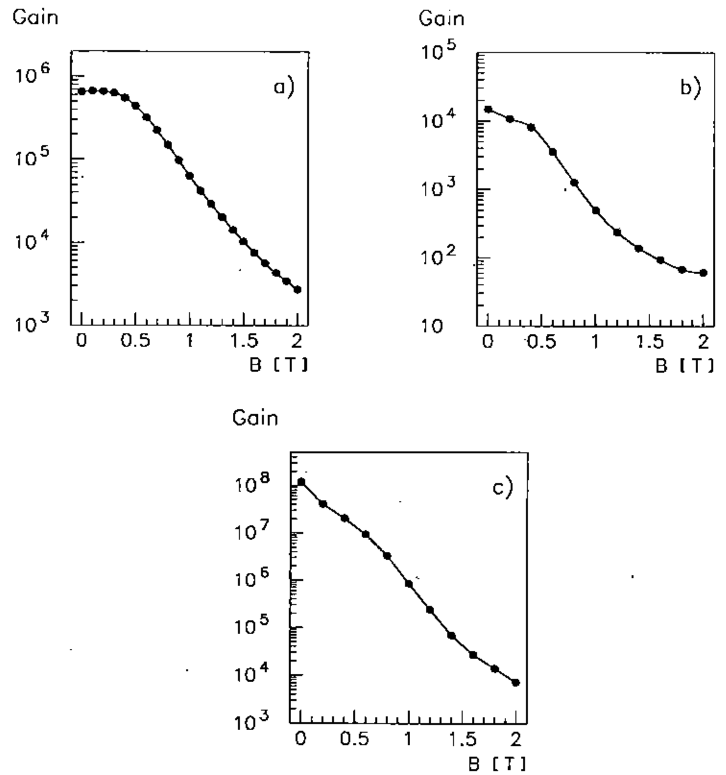

Figure 1: Gain of the fine mesh phototubes as a function of the magnetic field strength parallel to the tube axis. a) 1" tube, U = 2000V; b) 1.5 " tube, U = 2000V; c) 2 " tube, U = 2500 V

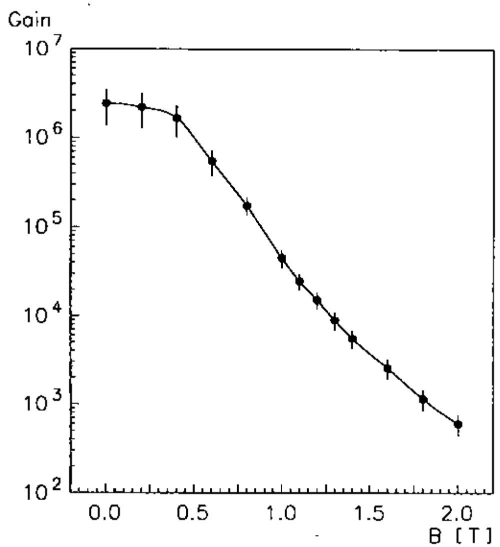

Figure 2: Average gain of four 1" phototubes (U = 2000 V) as a function of the magnetic field B. The length of the error bars indicates the variance of the sample.

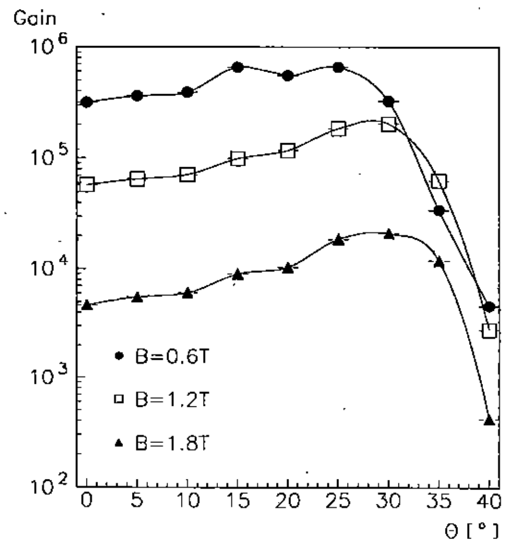

Figure 3: Gain of the 1" phototube as a function of the angle θ between the tube axis and the direction of the magnetic field for three different field strengths B. The full lines are included to guide the eye.

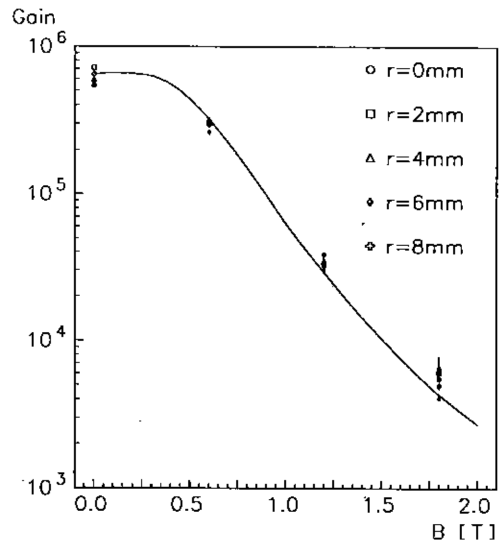

Figure 4: Gain of the 1" phototube as a function of the field strength B for different impact points of the photons on the cathode.

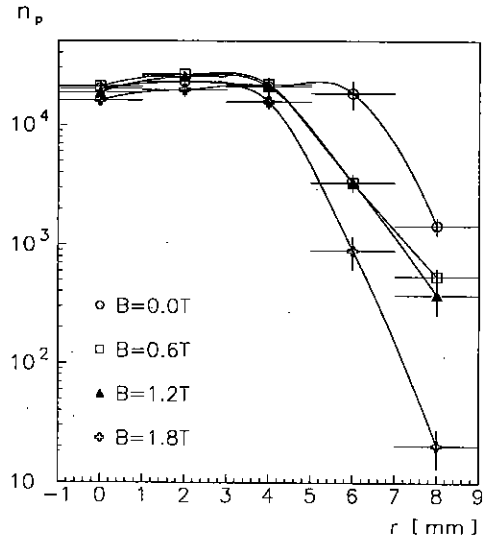

Figure 5: Number of photoelectrons for the 1" phototube as a function of distance of the impact point from the phototube axis for different field strength B.

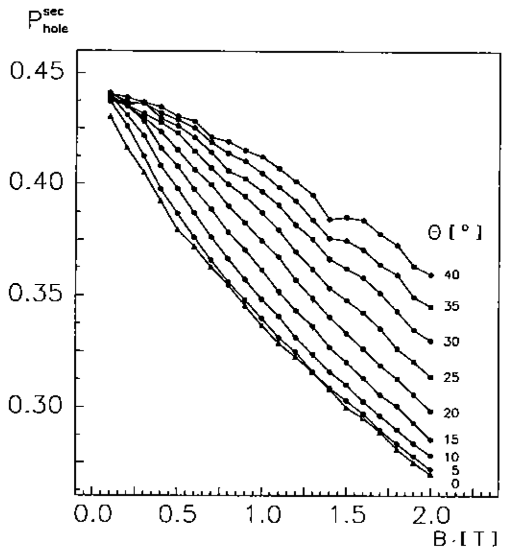

Figure 6: Probability P^{sec}_{hole} of a secondary electron to pass a hole of the mesh for different angles between the phototube axis and the magnetic field. The lines are shown to guide the eye.

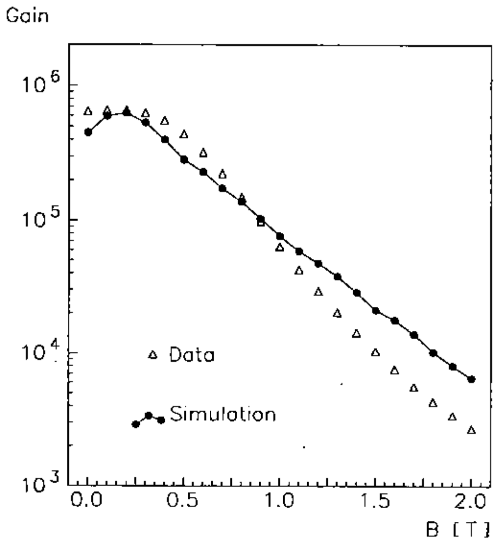

Figure 7: Comparison of measured and simulated gain of an 1" phototube as a function of the magnetic field B. The curves are normalized to each other at 0.2 Tesla.

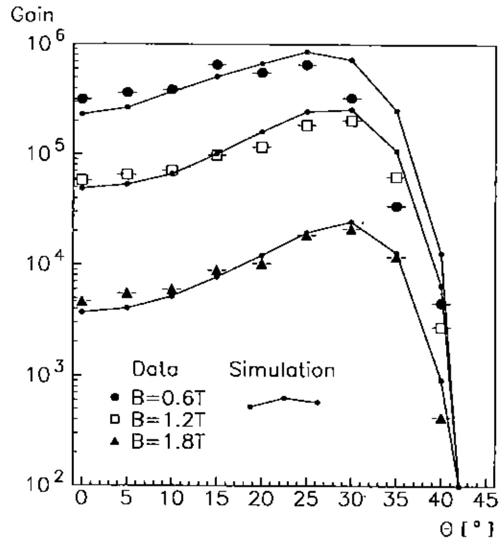

Figure 8: Measured and simulated (full line) gain of an 1" phototube as a function of the angle *θ* between the phototube axis and the magnetic field.